

Low-loss planar optical waveguides in strontium barium niobate crystals formed by ion-beam implantation

D. Kip and S. Aulkemeyer

Fachbereich Physik, Universität Osnabrück, 49069 Osnabrück, Germany

P. Moretti

Département de Physique de Matériaux, Université Claude Bernard Lyon 1, 69 622 Villeurbanne, France

Received February 15, 1995

Planar optical waveguides have been formed in strontium barium niobate single crystals by either proton or helium-ion implantation. The profiles of the ordinary and the extraordinary refractive indices are deduced from dark-line mode spectroscopy. Optical barriers with depths to $\Delta n_o = 2.6\%$ for protons and $\Delta n_e = 5.5\%$ for helium are obtained. By proton implantation we find a very low intensity loss of 0.4 cm^{-1} for ordinarily and a higher value of 2.7 cm^{-1} for extraordinarily polarized light at 632.8 nm . For helium-implanted waveguides both values are $\sim 4 \text{ cm}^{-1}$.

Strontium barium niobate single crystals ($\text{Sr}_{0.61}\text{Ba}_{0.39}\text{-Nb}_2\text{O}_6$; SBN) exhibit large electro-optic coefficients¹ and high photorefractive sensitivities.² For this reason SBN has many applications in optical data storage and optical data processing^{3,4} and is now close to utilization in commercial applications. Optical waveguides in this material may be used in combination with other components of integrated optics, e.g., laser diodes or optical fibers, thus providing cheap and easy-to-handle laser sources, which are of major importance in commercial optical systems. Such devices as light modulators with very low half-wave voltage use only the electro-optic properties of the material. In addition, the high light intensities that one can reach easily in waveguide structures in conjunction with excellent photorefractive properties permit several wave-mixing techniques such as beam coupling and phase conjugation.^{5,6}

Waveguide formation by sulfur diffusion into SBN crystals has been performed by Bulmer *et al.*,⁷ but the waveguides achieved exhibit high losses and small index changes. Helium implantation in SBN was mentioned briefly by Youden *et al.*⁸; however, no details of their results were given. Recently low-loss SBN waveguides were fabricated by a refractive-index increase because of the static strain-optic effect.⁹

Here we report the fabrication of planar waveguides in SBN crystals by proton and helium-ion implantation. This technique has been successfully applied to several ferroelectric oxide crystals, e.g., LiNbO_3 , KNbO_3 , and BaTiO_3 by the use of He^+ (Refs. 10–12) or H^+ (Ref. 13) ions. The implantation of light ions with high energy into oxide crystals results in the formation of a buried damaged layer that has a reduced refractive index compared with that of the substrate material.¹⁴ Nominally pure substrate material with z-cut geometry is used. Ordinary and extraordinary refractive-index profiles for different ion doses are obtained by mode spectroscopy. Because of the implantation process a broad increase in optical density is created in the visible region that is rather more pronounced for proton implantation than for helium-implanted samples. The loss of the wave-

guides is measured in dependence of wavelength and implanted dose.

We carried out the investigations with nominally pure SBN crystals. All samples were precisely polished for end-face coupling with dimensions of $2.5 \text{ mm} \times 5.0 \text{ mm}$ to $4.5 \text{ mm} \times 5.0 \text{ mm}$ and a thickness of 1 mm . The samples were irradiated at room temperature with H^+ ions at an energy of 1.0 MeV and doses of $(1, 2, 4, 6, 8) \times 10^{16} \text{ cm}^{-2}$ and He^+ ions at an energy of 2.0 MeV and doses of $(1, 2, 3, 6) \times 10^{16} \text{ cm}^{-2}$. During the implantation the temperature of the crystals was controlled by a combination of resistive heating and liquid- N_2 cooling, with the temperature stabilized to $\sim 30^\circ \text{C}$. To avoid channeling effects, we tilted the irradiated face of the z-cut crystal slightly with respect to the beam axis. The beam flux was $\sim 0.3 \mu\text{A cm}^{-2}$.

The waveguiding properties of the implanted samples were investigated by dark-line spectroscopy. We used a well-characterized rutile prism and a precise rotary stage to measure the effective refractive indices of the waveguides. Both TE and TM modes were excited by ordinarily and extraordinarily polarized light ($\lambda = 514.5 \text{ nm}$) propagating along the x direction. As an example, Fig. 1 shows the TM dark-line spectrum of the waveguide He2 (2.0 MeV He^+ , $2 \times 10^{16} \text{ cm}^{-2}$). From the measured effective refractive indices we calculate the corresponding refractive-index profiles by a least-squares fit algorithm that optimizes the parameters of an assumed analytical profile function.¹⁵

Optical density spectra were measured with a Cary 17D spectrometer. The results for ordinarily polarized light are shown in Fig. 2. For the He^+ -implanted samples we observe a small increase of the optical density, mainly in the range of $400\text{--}600 \text{ nm}$, whereas there is a more pronounced and broader increase for proton implantation that grows significantly with higher dose. This increase of optical density may be related both to light absorption by defects¹⁶ and to the creation of scattering centers¹⁷ by the implanted ions.

In Fig. 3 the extraordinary refractive-index profiles for the H^+ - and He^+ -implanted samples are shown.

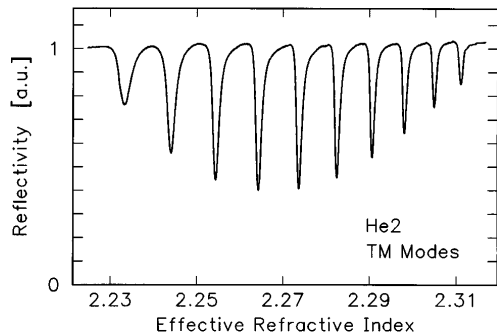


Fig. 1. Dark-line spectrum of the waveguide He2 (2.0-MeV He⁺, 2×10^{16} cm⁻²). The light polarization is extraordinary (TM modes), and the light propagates along the x direction.

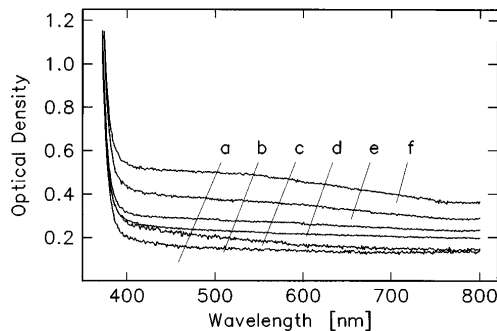


Fig. 2. Optical density spectra of implanted z-cut samples (1-mm thickness) for ordinarily polarized light: a, reference crystal (not implanted); b, 2.0-MeV He⁺ at a dose of 6×10^{16} cm⁻²; c, d, e, f, 1.0-MeV H⁺ at doses of (1, 2, 4, 8) $\times 10^{16}$ cm⁻², respectively.

The profiles of the ordinary refractive index are quite similar. The waveguide depth for He implantation is ~ 9.7 μm , and for proton implantation ~ 4.6 μm . These values are in fairly good agreement with TRIM¹⁸ calculations (9.2 and 4.4 μm , respectively). For the highest doses used in this research (8×10^{16} and 6×10^{16} cm⁻² for H⁺ and He⁺, respectively), optical barriers with depths to $\Delta n_e = 2.6\%$ and $\Delta n_o = 2.4\%$ with protons and $\Delta n_e = 5.5\%$ and $\Delta n_o = 4.6\%$ with He are obtained. For the He⁺-implanted waveguides we observe—independently of the light polarization—a strong lowering of the refractive index at the surface, related to the electronic damage process caused by the incident ions that increases with the deposited fluence. There are only small electronic effects for the proton-implanted samples.

The fitted ordinary refractive-index profiles of proton-implanted SBN yield a waveguide depth that increases slightly (from 9.5 to 10.4 μm) with the dose. At the moment we are not sure whether this has a physical origin or depends on the parameterized profile function (half Gaussian and half exponential with a plateau at the surface) that has been used for profile fitting. We applied also an inverse WKB method¹⁹ for reconstruction of the profiles. This yields nearly the same profile shapes and the same increasing depths of the implanted barriers.

We measured the loss of waveguides He3 (He⁺, 3×10^{16} cm⁻²) and H4 (H⁺, 4×10^{16} cm⁻²) by coupling light into and out of the end faces of the samples. The

light is focused by microscope lenses (magnifications 20 \times and 40 \times) onto the crystal to match the beam to the numerical aperture of the waveguide, and a cylindrical lens in front of the microscope lens ensures small beam divergence inside the sample. The light either is extraordinarily polarized, exciting TM modes, or has ordinary polarization to excite TE modes. Light propagation is along the x axis of the samples.

In Fig. 4 the results of the absorption measurements are shown for several laser lines of a He-Ne laser and an Ar-ion laser. To evaluate the measurements we estimated a launch efficiency of 80% (thus taking into account the imperfect aperture matching and crystal edge polishing) and corrected the data for Fresnel reflections. For proton implantation (waveguide H4) we obtained a low loss of 0.7 cm⁻¹ (0.4 cm⁻¹) for ordinarily polarized light and a higher value of 2.7 cm⁻¹ (2.8 cm⁻¹) for extraordinarily polarized light at a wavelength of $\lambda = 514.5$ nm (632.8 nm). For the He-implanted waveguide He3 no such significant dependence on polarization was found. In this case the losses are ~ 4 cm⁻¹, and the values for extraordinary

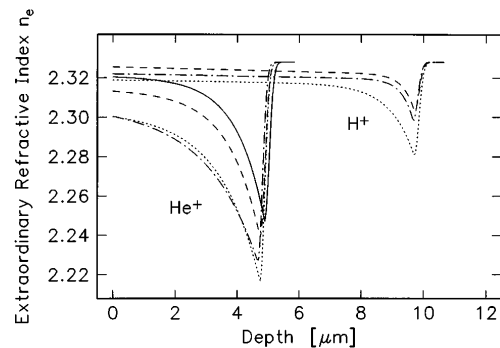


Fig. 3. Extraordinary refractive-index profiles of He⁺- and H⁺-implanted waveguides upon SBN substrates. The waveguide depth is ~ 4.6 μm for samples and ~ 9.7 μm for H⁺ implantations, and the substrate refractive index is $n_e = 2.330$. 2.0-MeV He⁺ and (1, 2, 3, 6) $\times 10^{16}$ cm⁻²; 1.0-MeV H⁺ and (2, 4, 8) $\times 10^{16}$ cm⁻².

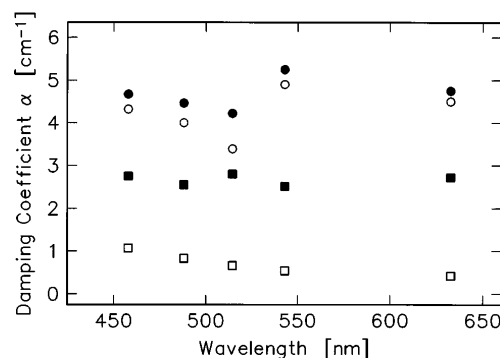


Fig. 4. Damping coefficients of the waveguides He3 (2.0-MeV He⁺, 3×10^{16} cm⁻²) and H4 (1.0-MeV H⁺, 4×10^{16} cm⁻²) measured by end-face coupling for several laser lines along the x direction of the crystal: He3, ordinary (○) and extraordinary (●) polarization; H4, ordinary (□) and extraordinary (■) polarization. All values are corrected for Fresnel reflections, and an efficiency of 80% for the end-face coupling has been assumed.

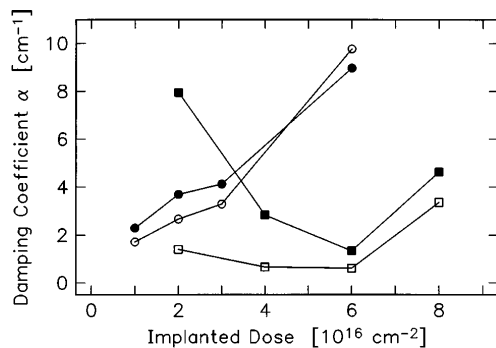


Fig. 5. Damping coefficients of He⁺- and H⁺-implanted waveguides relative to the implanted dose at a wavelength of 514.5 nm. He⁺, ordinary (○) and extraordinary (●) polarization; H⁺, ordinary (□) and extraordinary (■) polarization. All values are corrected for Fresnel reflections, and an efficiency of 80% for the end-face coupling has been assumed. The lines are merely guides for the eye.

light polarization are only slightly higher than for ordinarily polarized light.

The dependence of loss on the implanted dose is shown in Fig. 5. For the He-implanted waveguides we observe a strong increase of the damping coefficients for higher doses that may be related to the stronger electronic damage in these samples (see Fig. 3). A quite different behavior is measured for proton implantation. Here we find a minimum of loss for intermediate ion doses. This can be explained by the lowering of tunneling losses with increasing dose, followed by an ion-induced increase of (electronic) crystal damage for even higher doses.

From the comparatively low loss of the proton-implanted samples we can deduce that the broad increase of optical density is caused predominantly by light scattering or absorption in the implanted barrier rather than by damping in the waveguiding layer. Otherwise we would expect much higher optical damping coefficients of the waveguide.

In summary, planar optical waveguides in SBN crystals can be formed by proton and He-ion implantation. The multimode waveguides show sharp dark-line spectra and have very low damping coefficients, reaching values of 0.4 cm^{-1} for proton-implanted samples without any annealing treatment. These loss values are among the lowest reported for ion-implanted waveguides, permitting a wide spectrum of applications in integrated optics. An increase in the optical density found after implantation for the whole visible range of the spectrum can be related to absorption and light scattering in the implanted barrier and does not influence the properties of the waveguiding layer.

Annealing treatment of the waveguides provides a further reduction of loss,²⁰ and we plan to investigate this as well as to make quantitative measurements of the electro-optic and photorefractive properties.

Financial support of the Deutsche Forschungsgemeinschaft (grants SFB 225 and D9 and scholarship Ki 482/2-1) is gratefully acknowledged.

References

1. P. V. Lenzo, E. G. Spencer, and A. A. Ballman, *Appl. Phys. Lett.* **11**, 23 (1967).
2. K. Megumi, H. Kozuka, M. Kobayashi, and Y. Furuhashi, *Appl. Phys. Lett.* **30**, 631 (1977).
3. F. Micheron and G. Bismuth, *Appl. Phys. Lett.* **20**, 79 (1972).
4. P. Yeh and A. E. T. Chiou, *Opt. Lett.* **12**, 138 (1987).
5. M. Zha, D. Fluck, P. Günter, M. Fleuster, and C. Buchal, *Opt. Lett.* **18**, 577 (1993).
6. D. Kip and E. Krätzig, *Opt. Lett.* **17**, 1563 (1992).
7. C. H. Bulmer, O. Eknayan, H. F. Taylor, A. S. Greenblatt, L. A. Beech, and R. R. Neurgaonkar, *Proc. Soc. Photo-Opt. Instrum. Eng.* **704**, 208 (1986).
8. K. E. Youden, S. W. James, R. W. Eason, P. J. Chandler, L. Zhang, and P. D. Townsend, *Opt. Lett.* **17**, 1509 (1992).
9. J. M. Marx, Z. Tang, O. Eknayan, H. F. Taylor, and R. R. Neurgaonkar, *Appl. Phys. Lett.* **66**, 274 (1995).
10. G. L. Destefanis, J. P. Gailliard, E. L. Ligeon, S. Valette, B. W. Farmery, P. D. Townsend, and A. Perez, *J. Appl. Phys.* **50**, 7898 (1979).
11. T. Bremer, W. Heiland, B. Hellermann, P. Hertel, E. Krätzig, and D. Kollwe, *Ferroelectr. Lett.* **9**, 11 (1988).
12. P. Moretti, P. Thevenard, G. Godefroy, R. Sommerfeld, P. Hertel, and E. Krätzig, *Phys. Status Solidi A* **117**, K 85 (1990).
13. P. Moretti, P. Thevenard, K. Wirl, P. Hertel, H. Hesse, E. Krätzig, and G. Godefroy, *Ferroelectrics* **128**, 13 (1992).
14. P. D. Townsend, *Nucl. Instrum. Methods B* **65**, 243 (1992).
15. P. J. Chandler and F. L. Lama, *Opt. Acta* **33**, 127 (1986).
16. A. Garcia-Cabanes, J. A. Sanz-Garcia, M. Carbrera, F. Agullo-Lopez, C. Zalso, R. Pareja, K. Polgar, K. Raksanyi, and I. Fölvári, *Phys. Rev. B* **37**, 6085 (1988).
17. S. A. M. Al-Chalabi, B. L. Weiss, and K. P. Homewood, *Nucl. Instrum. Methods B* **28**, 255 (1987).
18. J. F. Ziegler, J. P. Biersack, and U. Littmark, *The Stopping and Ranges of Ions in Solids* (Pergamon, New York, 1988).
19. P. Hertel and H. P. Menzel, *Appl. Phys. B* **44**, 75 (1987).
20. J. Y. C. Wong, L. Zhang, G. Kakarantzas, P. D. Townsend, P. J. Chandler, and L. A. Boatner, *J. Appl. Phys.* **71**, 149 (1992).